Solubility of Gases and Liquids in Glassy Polymers

Maria Grazia De Angelis and Giulio C. Sarti

Dipartimento di Ingegneria Chimica, Mineraria e delle Tecnologie Ambientali, Università di Bologna, 40131 Bologna, Italy; email: giulio.sarti@unibo.it

Annu. Rev. Chem. Biomol. Eng. 2011. 2:97–120

First published online as a Review in Advance on January 11, 2011

The *Annual Review of Chemical and Biomolecular Engineering* is online at chembioeng.annualreviews.org

This article's doi:
10.1146/annurev-chembioeng-061010-114247

1947-5438/11/0715-0097$20.00

Keywords

nonequilibrium thermodynamic models, fractional free volume, sorption, glasses

Abstract

This review discusses a macroscopic thermodynamic procedure to calculate the solubility of gases, vapors, and liquids in glassy polymers that is based on the general procedure provided by the nonequilibrium thermodynamics for glassy polymers (NET-GP) method. Several examples are presented using various nonequilibrium (NE) models including lattice fluid (NELF), statistical associating fluid theory (NE-SAFT), and perturbed hard sphere chain (NE-PHSC). Particular applications illustrate the calculation of infinite-dilution solubility coefficients in different glassy polymers and the prediction of solubility isotherms for different gases and vapors in pure polymers as well as in polymer blends. The determination of model parameters is discussed, and the predictive abilities of the models are illustrated. Attention is also given to the solubility of gas mixtures and solubility isotherms in nanocomposite mixed matrices. The fractional free volume determined from solubility data can be used to correlate solute diffusivities in mixed matrices.

INTRODUCTION

The sorption of low-molecular-weight species in glassy polymers is a process of considerable interest in industrial practice in several applications such as membrane separations, solvent extraction, packaging, volatile organic compound detection, thin film coating, and environmental stress cracking.

In addition to the practical need for fluid sorption and desorption data in glassy polymer phases, a more fundamental issue arises from the nonequilibrium nature of glassy systems, which, at a given temperature, pressure, and external penetrant activity, absorb different amounts of fluid depending on their thermal, solvation, and mechanical history (1–4).

Therefore, the usual well-established tools based on equilibrium thermodynamics become inappropriate to describe the behavior of such systems. In rubbery polymers, true thermodynamic equilibrium is locally reached immediately, and one simply has to choose the proper equilibrium thermodynamic constitutive equation to represent the penetrant chemical potential in the polymeric phase, selecting between the activity coefficient approach (5–9) or equation-of-state (EoS) method (10–16) and using the most appropriate expression for the particular system.

Glassy polymers, however, are different insofar as the matrix is under nonequilibrium conditions and the usual thermodynamic results do not hold. Therefore, a different description must be used.

We review here some reliable methods to obtain solubility isotherms in glassy polymeric phases, with particular attention to the conditions needed for predictive calculations. In particular, we list briefly the methods based on molecular simulations and then present the main features of the empirical dual mode model, which is the most commonly used at present. Subsequently, we show in detail the main features of the nonequilibrium thermodynamics for glassy polymers (NET-GP) approach (17), namely, the general assumptions and results of the model, the procedure to calculate solubility isotherms of glassy phases, the EoS models that have been implemented to describe the behavior of mixtures, the significance and determination of the model parameters, the special cases of infinite-dilution solubility and solubility of liquid solutes, and finally several examples that illustrate the application of this method.

MODELS FOR THE SOLUBILITY OF GASES AND LIQUIDS IN GLASSY POLYMERS

Molecular Simulation–Based Approaches

A short description of molecular simulation–based approaches is given here; more details can be found elsewhere (18). In molecular simulations, the calculation of solubility in a glassy polymer phase relies on the same computational methods available for the evaluation of properties above the glass transition temperature, T_g, namely, the grand canonical Monte Carlo (GCMC) (19), Gibbs ensemble Monte Carlo (GEMC) (20), Widom test particle insertion (21), staged particle deletion (SPD) (22), and direct particle deletion (DPD) (23–25) methods. The simulation of any glassy polymer property is, however, restricted because the characteristic relaxation times exceed by far the longest time and length scales that current computers can simulate. It is thus difficult to generate a realistic configuration of the polymer glass (26). At high pressures, one also must consider that the sorption of gas molecules is accompanied by swelling of the polymer matrix, which is due in part to relaxation and requires slow rearrangement of the polymer chains. Some authors have introduced the use of preswollen or preloaded packing models to represent high-concentration states of polymer/penetrant systems (24, 27, 28).

Despite the great advances made in the past decade in the development of algorithms, the computational time required to evaluate gas or liquid solubility in a glassy polymer is not yet comparable with that required by macroscopic approaches such as EoS models. Interesting synergies, however, can be envisioned by combining microscopic and macroscopic methods, as molecular simulations can provide information on the structure of the polymer and on macroscopic properties that are otherwise unavailable to macroscopic models or experimentally inaccessible (29).

Dual-Mode Sorption Model

The most widespread description of fluid solubility in glassy polymers is the dual-mode sorption (DMS) model (30, 31); the straightforwardness of its use for data fitting apparently makes it difficult to replace. The DMS picture has a phenomenological basis, as it assumes that two populations of penetrant molecules are sorbed in the polymeric solid. The first one is dissolved in the bulk polymer matrix and is linear with pressure through Henry's law, whereas the second one, described by a Langmuir adsorption isotherm, is adsorbed onto the surface of the microvoids that are considered to be present in the polymer as a consequence of the excess free volume frozen into the glassy matrix. The resulting overall concentration of the penetrant, C, as a function of the external gas pressure, p, is

$$C = K_D p + \frac{C'_H b p}{1 + b p}. \qquad 1.$$

The parameters C'_H and b are the Langmuir capacity and hole affinity parameter, respectively. C'_H can be related to the nonequilibrium properties of the mixture through the excess free volume distribution (32), whereas the equilibrium parameter K_D (Henry's constant) can be related to the dilation of the polymer owing to the sorption process (33) and calculated by an EoS procedure (32).

The DMS model exhibits the typical limitations of empirical models: The parameters must be evaluated for each polymer-penetrant system at each temperature by best fitting Equation 1 to experimental solubility isotherms, the parameters used for sorption differ from those needed to describe desorption, and the values of the dual mode parameters are strongly dependent on the pressure range of the sorption data (34).

Nonequilibrium Thermodynamics of Glassy Polymers

The main features of the macroscopic nonequilibrium approach for the solubility in glassy polymers are described below.

General considerations. In the early 1990s, several studies aimed to develop a more fundamental approach than that of the DMS model (35–38) by using suitable statistical thermodynamic expressions for the Gibbs free energy of the glassy mixture (39). The nonequilibrium properties of the glassy state are accounted for by making use of an appropriate order parameter: the fractional free volume (FFV) of the polymer at T_g, which is frozen into the system for all temperatures below T_g, or the number of holes per polymer mass (36, 37).

In the NET-GP approach a relationship is derived between the thermodynamic properties above and below T_g, i.e., between equilibrium and pseudoequilibrium conditions (17). The latter are asymptotically reached by the glassy phase when the temperature, pressure, and stress as well as the fugacity of all components in the external phase are kept constant; however, owing to the

departure from equilibrium, the pseudoequilibrium conditions depend on the thermomechanical history of the material.

In NET-GP analysis, the glassy polymer–penetrant phases are assumed homogeneous and amorphous, and their state is characterized by the classical macroscopic variables, i.e., temperature T, pressure p, and composition, with the addition of order parameters accounting for the departure from equilibrium. In isotropic conditions, the density of the polymer species, ρ_{pol}, is sufficient to determine the departure from equilibrium and is chosen as the proper order parameter. The hindered mobility of the glassy polymer chains freezes the material into a nonequilibrium state that can be described by the difference between the observed polymer density ρ_{pol} and its equilibrium value at the given T, p, and mixture composition ρ_{pol}^{EQ}. As a result, all thermodynamic functions, for example the Helmholtz free energy density a^{NE}, are given by an equation of the type (17)

$$a^{NE} = a^{NE}(T, p, \Omega_i, \rho_{pol}), \qquad 2.$$

where Ω_i is the mass ratio of solute i to polymer. Considering the order parameter ρ_{pol} as an internal state variable for the system, and application of the theory of materials endowed with internal state variables (40) the nonequilibrium Helmholtz free energy density of the glassy phase, a^{NE}, was shown to depend only on temperature, polymer mass density, and composition, and is independent of pressure (17):

$$\left(\frac{\partial a^{NE}}{\partial p}\right)_{T,\rho_i,\rho_{pol}} = 0. \qquad 3.$$

The chemical potential per unit mass of penetrant i dissolved in the glassy phase is given by

$$\mu_i^{NE} = \left(\frac{\partial G^{NE}}{\partial m_i}\right)_{T,p,m_{j\neq i},m_{pol}} = \left(\frac{\partial a^{NE}}{\partial \rho_i}\right)_{T,p,\rho_{j\neq i},\rho_{pol}}, \qquad 4.$$

where G^{NE} is the total Gibbs free energy of the mixture; m_{pol} and m_i are the masses of polymer and of penetrant i, respectively; and ρ_i is the density of the i-th penetrant.

As a direct consequence of Equation 3, a^{NE}, in a general nonequilibrium state, coincides with the corresponding property a^{EQ} obtained from the equilibrium curve at the same T, ρ_{pol}, and Ω_i:

$$a^{NE}(T, p, \Omega_i, \rho_{pol}) = a^{EQ}(T, \Omega_i, \rho_{pol}). \qquad 5.$$

Similarly, the chemical potential per unit mass of solute i in the glassy phase is given by

$$\mu_i^{NE}(T, p, \Omega_i, \rho_{pol}) = \mu_i^{EQ}(T, \Omega_i, \rho_{pol}). \qquad 6.$$

Therefore, once an expression for a^{EQ} is selected for the polymer-penetrant mixture, the corresponding nonequilibrium equation is readily obtained through the simple relationships in Equations 5 and 6. Such results are derived in general terms and are independent of the particular EoS model used to evaluate the free energy.

Free energy functions are given by different EoS models such as lattice fluid (LF) (12, 41, 42), statistical associating fluid theory (SAFT) (13, 43, 44), and perturbed hard sphere chain (PHSC) (14–16, 45). These models give rise to corresponding nonequilibrium (NE) models known as NELF (46), NE-SAFT (17, 47), and NE-PHSC (48), respectively. The nonequilibrium information is represented by the value of ρ_{pol}, which must be measured experimentally and cannot be calculated from the equilibrium EoS.

Gas and liquid solubility calculation. In the case of true thermodynamic phase equilibrium, solubility is evaluated by equating the equilibrium chemical potential of the j-th penetrant in the polymer phase ($\mu_j^{EQ(s)}$) to that in the external fluid phase ($\mu_j^{EQ(f)}$), using the equilibrium polymer density given by the EoS at that T, p, and composition.

For solubility in a glassy phase, the polymer density does not match its equilibrium value, ρ_{pol}^{EQ}; however, NET-GP results show that a pseudoequilibrium condition is reached when the chemical potential of the penetrant in the glassy mixture, at T, p, and a fixed polymer density, equals the corresponding chemical potential of the penetrant in the external phase (17):

$$\mu_j^{NE(s)}(T, p, \Omega_j, \rho_{pol}) = \mu_j^{EQ(f)}(T, p). \quad 7.$$

In Equation 7 the nonequilibrium solute chemical potential is calculated using Equation 4 after an appropriate EoS for the polymer-penetrant system has been selected.

The pseudoequilibrium content of penetrant j in the polymer, Ω_j, can be calculated if the pseudoequilibrium polymer density, ρ_{pol}, is known; that value represents a crucial input for the nonequilibrium approach, as usually all nonequilibrium models are sensitive to polymer density.

The polymer density value during sorption is normally not available at all penetrant activities, which is a constraint for the application of the NET-GP approach as a completely predictive tool. In several cases of practical interest, such as for low values of activity with respect to saturated liquid, or for solutes with extremely low solubility, the density of the pure glass, ρ_{pol}^0, provides a good estimate of the polymer density, ρ_{pol}. In such cases, the NET-GP approach can be applied in a predictive way.

When swelling agents or high gas pressures are used, the NET-GP approach needs some further consideration. In particular the polymer density during gas sorption varies linearly with penetrant pressure (32, 33, 50),

$$\rho_{pol}(p) = \rho_{pol}^0(1 - k_{sw}p), \quad 8.$$

where the swelling coefficient, k_{sw}, represents the effect of gas pressure on glassy polymer density. This coefficient is a nonequilibrium parameter that depends on the thermomechanical and sorption history of the sample. The value of the swelling coefficient, k_{sw}, can be obtained, in principle, from a single experimental solubility datum at high pressure for the system under consideration, using Equations 7 and 8 (50).

At infinite dilution, the phase equilibrium condition represented by Equation 7 can be solved for the solubility coefficient using the LF model. The infinite dilution solubility coefficient, S_0, expressed in [cm^3 of gas (STP)]/[(cm^3 of polymer) (atm)], is the initial slope of the solubility isotherm:

$$S_0 = \lim_{p \to 0} \frac{C}{p}. \quad 9.$$

The explicit expression for S_0 of a penetrant (labeled by subscript 1) in a polymer (labeled by subscript 2) as a function of T, ρ_{pol}^0, pure polymer and pure penetrant characteristic parameters, and the binary interaction parameter k_{12}, which enters the model mixing rule and accounts for deviations of the binary interaction energy from the geometric mean rule, is given by (50)

$$\ln S_0 = \ln\left(\frac{T_{STP}}{p_{STP}T}\right) + r_1^0\left\{\left[1 + \left(\frac{v_1^*}{v_2^*} - 1\right)\frac{\rho_{pol}^*}{\rho_{pol}^0}\right]\ln\left(1 - \frac{\rho_{pol}^0}{\rho_{pol}^*}\right) + \left(\frac{v_1^*}{v_2^*} - 1\right) + \frac{\rho_{pol}^0}{\rho_{pol}^*}\frac{T_1^*}{T}\frac{2}{p_1^*}(1 - k_{12})\sqrt{p_1^* p_2^*}\right\}, \quad 10.$$

where T_{STP} and p_{STP} are the standard temperature and pressure. In the expression between braces, the first two terms derive from the excess entropy term of the Gibbs free energy of the mixture and represent the entropic contribution to solubility, $\Phi^{(S)}$ (51), whereas the last term represents the enthalpic contribution, $\Phi^{(H)}$ (51), and contains the binary interaction parameter k_{12} between polymer 1 and penetrant 2. The entropic contribution is essentially related to fractional free

volume with respect to the close-packed state, $(1-\rho^0_{pol}/\rho^*_{pol})$, whereas the energetic contribution is directly related to the solubility parameter[1] of polymer and penetrant in equilibrium conditions, according to the usual relationships (51). The enthalpic and entropic contributions may also be associated directly with the enthalpy and entropy of solvation of the penetrant in the polymer at infinite dilution.

A different insight into the role of the different physical mechanisms is gained by considering that the dissolution is composed of three steps as follows: (*a*) condensation of the pure gas to the hypothetical liquid state with a molar volume equal to the partial molar volume existing in the equilibrium condensed mixture at infinite dilution, $\bar{V}_{1,EQ}$, at the same T and p; (*b*) dissolution of the condensed gas into the polymer, which leads to an equilibrium rubbery mixture; and (*c*) evolution from a rubbery equilibrium mixture to a nonequilibrium glassy phase characterized by the same T, p, and composition but with a different density equal to the density measured in the glass (52).

According to that three-step path, it is possible to elucidate the contributions of condensation, Φ_{cond}; equilibrium mixing, Φ^{EQ}_{mix}; and departure from equilibrium, Φ^{NE}, to the infinite dilution solubility value:

$$\ln(S_0) = \ln\left(\frac{T_{STP}}{p_{STP}T}\right) + \Phi^{NE} + \Phi^{EQ}_{mix} + \Phi_{cond}. \qquad 11.$$

The various contributions can be evaluated using the LF and NELF models, as described in more detail elsewhere (52).

The solubility of liquid molecules in glassy polymers also can be evaluated using the general results of the NET-GP model without any adaptation of the method or of the parameters. Recently, this method has been applied to some mixtures of liquids in glassy polymers (53). The model can be used in a straightforward way for the cases in which volume swelling is negligible; if the liquid penetrant gives rise to a non-negligible swelling, however, one can adjust the value of k_{sw} based on experimental sorption data in the high pressure range, or use the assumption of volume additivity between pure glassy polymer and pure liquid penetrant to obtain a possibly overestimated prediction.

EoS models. Different EoS, in particular the LF (12, 41, 42), SAFT (13, 43, 44), and PHSC (14–16, 45) models, have been profitably used for solubility calculations. Such models have been employed owing to their sound theoretical basis and their ability to represent the equilibrium properties of pure substances and fluid mixtures in the condensed phase. The solubility isotherms of fluids in glassy polymeric phases were obtained by using their extensions to nonequilibrium phases (NELF, NE-SAFT, NE-PHSC) for the glassy state (17). Detailed descriptions of the various parameters used in the models can be found in the references of the original papers.

Determination of the pure component parameters. The pure component parameters for the EoS model chosen are obtained by fitting the EoS calculations to the pure component equilibrium data. For the penetrant, volumetric and/or vapor pressure values are frequently available to that aim. For the polymer, one can use volumetric data as a function of temperature and pressure above T_g, data that are frequently available in the open literature and in some compilations (54), for the common case in which the rubbery phase can be reached experimentally. An example of such a procedure is shown in **Figure 1*a***: Volumetric data above and below T_g are given for polycarbonate

[1]Indeed, in the LF model the solubility parameter of a pure component is $\delta_i = \frac{\rho_i}{\rho_i^*}\sqrt{p_i^*}$ (51).

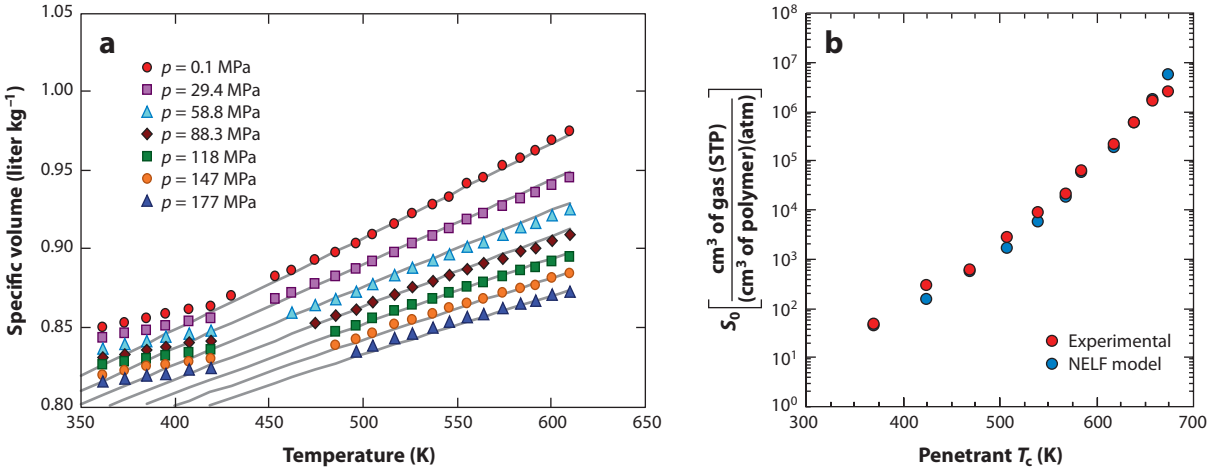

Figure 1

(*a*) Volumetric data for polycarbonate and comparison with statistical associating fluid theory (SAFT) equation-of-state (EoS) predictions. Experimental data are taken from Zoller & Walsh (54). STP, standard temperature and pressure. (*b*) Comparison between experimental (56) and nonequilibrium lattice fluid (NELF)-calculated values of the infinite dilution solubility coefficient S_0 of *n*-alkanes (from *n*-C_3 to *n*-C_{13}) at 35°C in poly[(trimethylsilyl) norbornene] (PTMSN), as a function of penetrant T_C. The calculated values were obtained with the LF parameters listed in **Table 1** and $k_{ij} = 0.0$ for all penetrants. Adapted from Reference 57.

(PC), and the SAFT model is used to fit the data above T_g. The resulting parameters for the SAFT model are $\sigma = 3.043$ Å, $M/m = 25.00$ g mol^{-1}, and $u_0/k = 371$ K.

There are, however, many polymers of particular interest for application in membrane separations, such as certain polyimides, polyacetylenes, and polynorbornenes, for which the polymer cannot reach T_g without chemical degradation or T_g is too high to investigate the rubbery region experimentally. In such cases, one can conduct a molecular simulation of the equilibrium polymeric phase above T_g, a technique whose general applicability is still under study (29), or use mixture rather than pure polymer data. One reliable method to evaluate polymer parameters when T_g cannot be reached is to use solubility coefficients in the polymer at infinite dilution for at least three gaseous penetrants, and fit them with Equation 10.

An example is given in **Figure 1*b***, which shows the fitting of the characteristic LF EoS parameters of the addition polymer poly[(trimethylsilyl) norbornene] (PTMSN) (55–57) using the experimental infinite dilution solubility values of various alkane penetrants (from C_3 to *n*-C_{13}) at 35°C in order to retrieve the pure polymer parameters for PTMSN. The binary interaction parameter, k_{ij}, was kept fixed at its first-order estimate (0.00), the pure polymer density was 0.883 kg liter^{-1}, and the characteristic parameters obtained are listed in **Table 1** (57).

Determination of the model binary interaction parameters. All mixture models for free energy also have one k_{ij} associated with each pair *i,j* of chemical species. This parameter can be obtained separately, e.g., from gas-polymer equilibrium data in the rubbery phase, when available. In the absence of any direct experimental information, the first-order approximation can be used for k_{ij} or, alternatively, it can be treated as an adjustable parameter, as is often done in thermodynamic studies of liquid-vapor equilibria. For mixtures formed by components of similar chemical structure, k_{ij} is essentially equal to 0.0 (regular solution behavior). For a homologous series of penetrants in the same polymeric phase, k_{ij} is often the same for all penetrants;

Table 1 Pure component equation-of-state (EoS) characteristic parameters

Lattice fluid EoS pure component parameters							
Polymer	**p^* (MPa)**	**T^* (K)**	**ρ^* (kg liter^{-1})**	**Penetrant**	**p^* (MPa)**	**T^* (K)**	**ρ^* (kg liter^{-1})**
PC (46)	534	755	1.275	CH_4 (59)	250	215	0.500
TMPC (47)	446	762	1.174	C_2H_4 (47)	345	295	0.680
BCPC (47)	531	794	1.480	*n*-C_4 (84)	290	430	0.720
PMMA (51)	560	695	1.270	*n*-C_5 (84)	305	451	0.749
PS (51)	360	750	1.099	CO_2 (46)	630	300	1.515
PSf (51)	600	830	1.310	H_2O (51)	2400	670	1.050
PPO (51)	479	739	1.177	CH_3OH	1080	510	0.900
PTMSN (57)	360	406	1.345	C_2H_5OH (51)	880	470	0.915
PTMSP (84)	416	405	1.250				
AF1600 (59)	280	575	2.16				
AF2400 (59)	250	624	2.13				
Statistical associating fluid theory EoS pure component parameters (47)							
Polymer	**σ (Å)**	**MW m^{-1} (g mol^{-1})**	**$u_0\,k^{-1}$ (K)**	**Penetrant**	**σ (Å)**	**MW m^{-1} (g mol^{-1})**	**$u_0\,k^{-1}$ (K)**
PSf	3.049	25.67	410.0	CO_2	3.171	31.05	216.08
PPO	3.043	24.01	320.0	N_2	3.575	28.01	123.53
PEMA	3.049	22.98	320.0	CH_4	3.700	16.01	190.29
Perturbed hard sphere chain-square well EoS pure component parameters (47)							
Polymer	**σ (Å)**	**MW m^{-1} (g mol^{-1})**	**$u_0\,k^{-1}$ (K)**	**Penetrant**	**σ (Å)**	**MW m^{-1} (g mol^{-1})**	**$u_0\,k^{-1}$ (K)**
PMMA	3.583	37.6	366.9	N_2	3.520	27.62	108
PEMA	3.450	32.78	290.5	CH_4	3.672	16.01	164.9
PSf	3.484	37.45	352	CO_2	2.484	16.26	145.11
PPO	3.600	37.73	293.0				

Abbreviations: PC, polycarbonate; TMPC, tetramethyl polycarbonate; BCPC, (bisphenol-chloral) polycarbonate; PMMA, poly(methyl methacrylate); PS, polystyrene; PSf, polysulfone; PPO, poly(phenylene oxide); PTMSN, poly[(trimethylsilyl) norbornene]; PTMSP, poly[1-(trimethylsilyl)-1-propyne]; PEMA, poly(ethyl methacrylate).

examples include the solubility of *n*-alkanes in fluorinated polymers and the solubility of fluorinated penetrants in hydrocarbon polymers, for which k_{ij} is in all cases close to 0.10 (58–60).

COMPARISON BETWEEN NONEQUILIBRIUM THERMODYNAMICS OF GLASSY POLYMERS MODEL RESULTS AND SOLUBILITY DATA

This section reviews the predictive ability of the procedure presented above using the PHSC, SAFT, and LF EoS as reference equilibrium models. To this aim, gas and liquid solubility data in different polymers are compared with the model predictions, following the pure predictive or correlative mode. In the case of glassy mixtures, the dry polymer density that has been used in the simulation is also specified. To test the behavior of the model in a variety of conditions, different mixtures and types of miscibility data are examined, including ternary solutions formed by a single gas in a polymer blend or by mixed gases in a single polymer. The data relative to the glassy systems are classified based on the swelling behavior of the penetrant, treating separately the nonswelling solutes such as N_2, O_2, and CH_4, and the swelling penetrants for which the calculation procedure is substantially different in nonequilibrium conditions. The case of mixed matrix membranes based on glassy polymers is also considered.

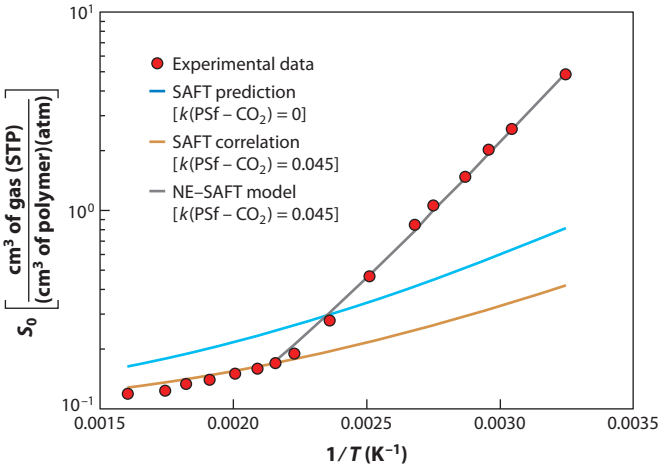

Figure 2

Solubility coefficient of CO_2 in polysulfone (PSf) at infinite dilution reported as a function of reciprocal temperature. The correlation with the statistical associating fluid theory (SAFT) equation of state (EoS) in the equilibrium range and with the nonequilibrium NE-SAFT model in nonequilibrium conditions are reported using the same binary interaction parameter $k_{ij} = 0.045$; the dotted line indicates equilibrium SAFT EoS calculations with $k_{ij} = 0.0$. STP, standard temperature and pressure.

Infinite Dilution Solubility Coefficient Above and Below the Glass Transition Temperature

The behavior of the NET-GP procedure is tested on a gas-polymer mixture whose solubility has been measured in both equilibrium (above T_g) and nonequilibrium (below T_g) conditions. In **Figure 2** the infinite dilution solubility coefficient of CO_2 in polysulfone (PSf) is plotted as a function of the inverse absolute temperature. Because the polymer dilation is negligible at low pressure, the polymer density is constant and equal to ρ^0_{pol}. In a semilog plot, the experimental sorption data above and below T_g lie on two lines characterized by different slopes; the glassy phase is characterized by a stronger temperature dependency of the gas solubility. In **Figure 2**, the predictions of both the SAFT EoS and the corresponding NE-SAFT model are presented and compared with experimental data for CO_2 in PSf. The same value of k_{ij} (0.045) fits the experimental data above T_g using SAFT and, using NE- SAFT, below T_g, where the equilibrium model would provide a large underestimation.

The value of ρ^0_{pol} was obtained at each temperature by considering the experimental density at T_g (≈180°C) to be 1.195 kg liter^{-1} and adopting a cubic thermal expansion coefficient equal to 2.0×10^{-4} K^{-1}. All the parameters used are listed in **Table 1**.

Infinite Dilution Solubility in Glassy Polymers and Correlations with Penetrant Parameters

Gas solubility in liquids and in rubbery polymers is often correlated with measures of gas condensability such as T_C using relations of the type (61, 62):

$$\ln(S_0) = a + b\,T_C. \qquad 12.$$

The intercept a and the slope b in Equation 12 are used empirically as adjustable constants; the values of b are similar for all liquid solvents and vary between 14 and 19 $\times 10^{-3}$ K^{-1} for different

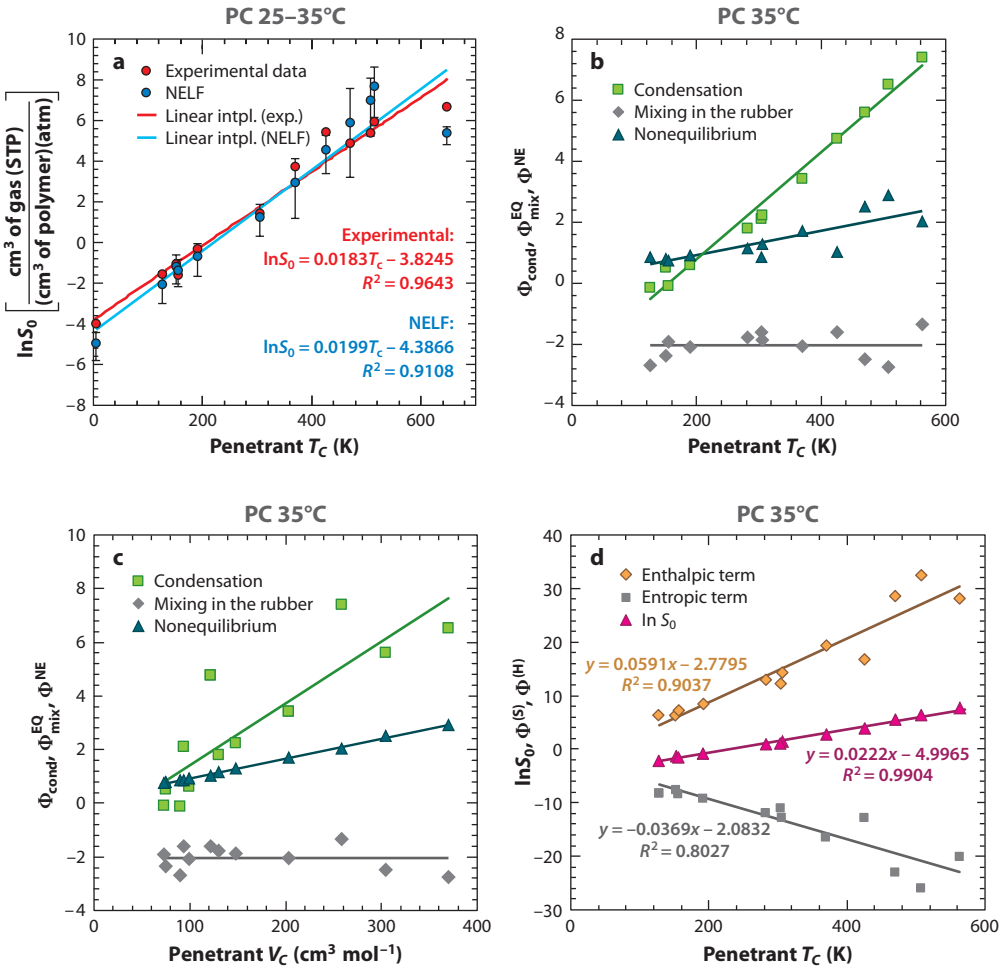

Figure 3

(*a*) Experimental and nonequilibrium lattice fluid (NELF)-predicted values of $\ln(S_0)$ of various penetrants in polycarbonate (PC) at 25°C–35°C (adapted from 51). intpl, interpolation. (*b*) Calculated values of Φ_{cond}, Φ^{EQ}_{mix}, and Φ^{NE} for PC at 35°C as a function of penetrant T_C (adapted from 52). (*c*) Calculated values of Φ_{cond}, Φ^{EQ}_{mix}, and Φ^{NE} for PC at 35°C as a function of critical molar volume V_C (adapted from 52). (*d*) Calculated values of S_0, the entropic term $\Phi^{(S)}$, and the enthalpic term $\Phi^{(H)}$ as a function of penetrant T_C for PC at 35°C (adapted from 51).

organic liquids (63). The use of such a linear relationship in correlating gas solubility in rubbers (64, 65) and glasses (66–68) has yielded values of parameter b similar to those observed in liquids. Gee (69) provided a simple theoretical framework for the observed correlation in rubbery polymers but none for glassy polymers.

For glassy polymers such as PC, poly(methyl methacrylate) (PMMA), poly(phenylene oxide) (PPO) and PSf, Equation 10 correctly describes the experimental infinite-dilution solubility data of many gases and vapors (51). In **Figure 3*a*** we compare NELF predictions and experimental data for the solubility coefficient in PC of a series of solutes (Ar, N_2, O_2, He, CO_2, CH_4, C_3H_8, and C_3H_6O at 35°C; SO_2 at 25°C; and n-C_5H_{12}, C_2H_5OH, and H_2O at 30°C) (51). The default value of $k_{ij} = 0.0$ was used in all cases. Similar good agreement was observed for PSf, PMMA, and PPO.

Further insight was obtained by calculating the contributions of condensation, Φ_{cond}; equilibrium mixing, Φ_{mix}^{EQ}; and nonequilibrium degree, Φ^{NE}, using a series of gas and vapor penetrants (Ar, N_2, O_2, CO_2, CH_4, C_2H_4, C_2H_6, C_3H_8, *n*-C_5H_{12}, *n*-C_6H_{14}, SO_2, and benzene) at 35°C, in the above-mentioned polymers. The results obtained by plotting Φ_{cond}, Φ_{mix}^{EQ}, and Φ^{NE} for the selected list of penetrants in PC as a function of T_C are shown in **Figure 3*b***. For any solute, Φ_{cond} is the same for all polymers because the reduced liquid density of each penetrant is the same for all matrices; the only polymer-dependent term is the liquid molar density that is taken from the partial molar volume. In particular, for the penetrants considered in PC, one finds that (52)

$$\Phi_{cond} = -2.73 + 0.0175T_C \quad (R^2 = 0.982). \qquad 13.$$

Clearly, the slope of the straight line interpolating Φ_{cond} and T_C is close to the value of 0.019 K^{-1} estimated by Gee (69). The intercept has a negative value, which indicates that the condensation term lowers the solubility of poorly condensable penetrants (e.g., $T_C < 156$ K) in the polymer.

As shown in **Figure 3*b***, the equilibrium mixing term, Φ_{mix}^{EQ}, is always negative and has the effect of lowering the solubility; its value is essentially constant with penetrant type. Because the nonequilibrium term, Φ^{NE}, is always positive, it increases the solubility with respect to the value obtained in the corresponding hypothetical rubbery polymer. In general, the value of Φ^{NE} increases with increasing penetrant T_C much more weakly than does the condensation term, and its intercept seems to be related to the FFV of the polymer. For the less condensable penetrants, $\Phi^{NE} > \Phi_{cond}$, i.e., the solubility enhancement produced by the excess FFV of the glassy polymer is greater than the solubility reduction associated with the unfavorable condensation term (52).

A similar analysis allows us to inspect the possible effect on the infinite-dilution solubility coefficient of molecular size as embodied by the critical molar volume V_C. The values of Φ_{cond}, Φ_{mix}^{EQ}, and Φ^{NE} for the various penetrants in PC versus V_C at 35°C are plotted in **Figure 3*c*** (52).

An alternative description is also obtained by considering the infinite dilution solubility as the sum of an energetic and an entropic contribution directly derived from the Gibbs free energy of the polymer-penetrant mixture. In particular, in **Figure 3*d*** one can see that the enthalpic term, $\Phi^{(H)}$, increases with T_C because the sorption enthalpy is mainly due to solute condensation; the entropic term, $\Phi^{(S)}$, however, decreases with increasing T_C owing to the larger size of more condensable penetrants that have a lower number of possible configurations available. Moreover, $\Phi^{(H)}$ is in general higher than $\Phi^{(S)}$, which gives rise to the observed linear positive correlation between $\ln S_0$ and T_C (51).

Solubility Isotherms of Nonswelling Gases in Glassy Polymers

The sorption isotherms of CH_4 in PPO and PSf, as well as the sorption isotherm of N_2 in poly(ethyl methacrylate) (PEMA) at 35°C (70), were considered as typical examples of nonswelling penetrants in glassy polymers. In the practical absence of polymer dilation, beyond the pure component parameters and k_{ij}, only the unpenetrated polymer density is required for a complete description of the solubility isotherms through the NET-GP approach. The pure component parameters for the different models used are listed in **Table 1**. The dry polymer density for PEMA at 35°C extrapolated from volumetric data is $\rho_{pol}^0 = 1.120$ kg liter^{-1}, whereas for PPO the dry polymer density is 1.063 kg liter^{-1} and for PSf 1.230 kg liter^{-1}. The k_{ij} values that best fit the low-pressure solubility data for the N_2-PEMA system are 0.020, −0.018, and 0.030 when using the SAFT, PHSC-SW, and LF models, respectively. For the CH_4-PSf system, k_{ij} is −0.015, −0.085, and −0.030 for the three different models, whereas for CH_4 in PPO k_{ij} is 0.00, −0.085, and −0.060 (47). The experimental data and the model calculations are shown in **Figure 4*a***.

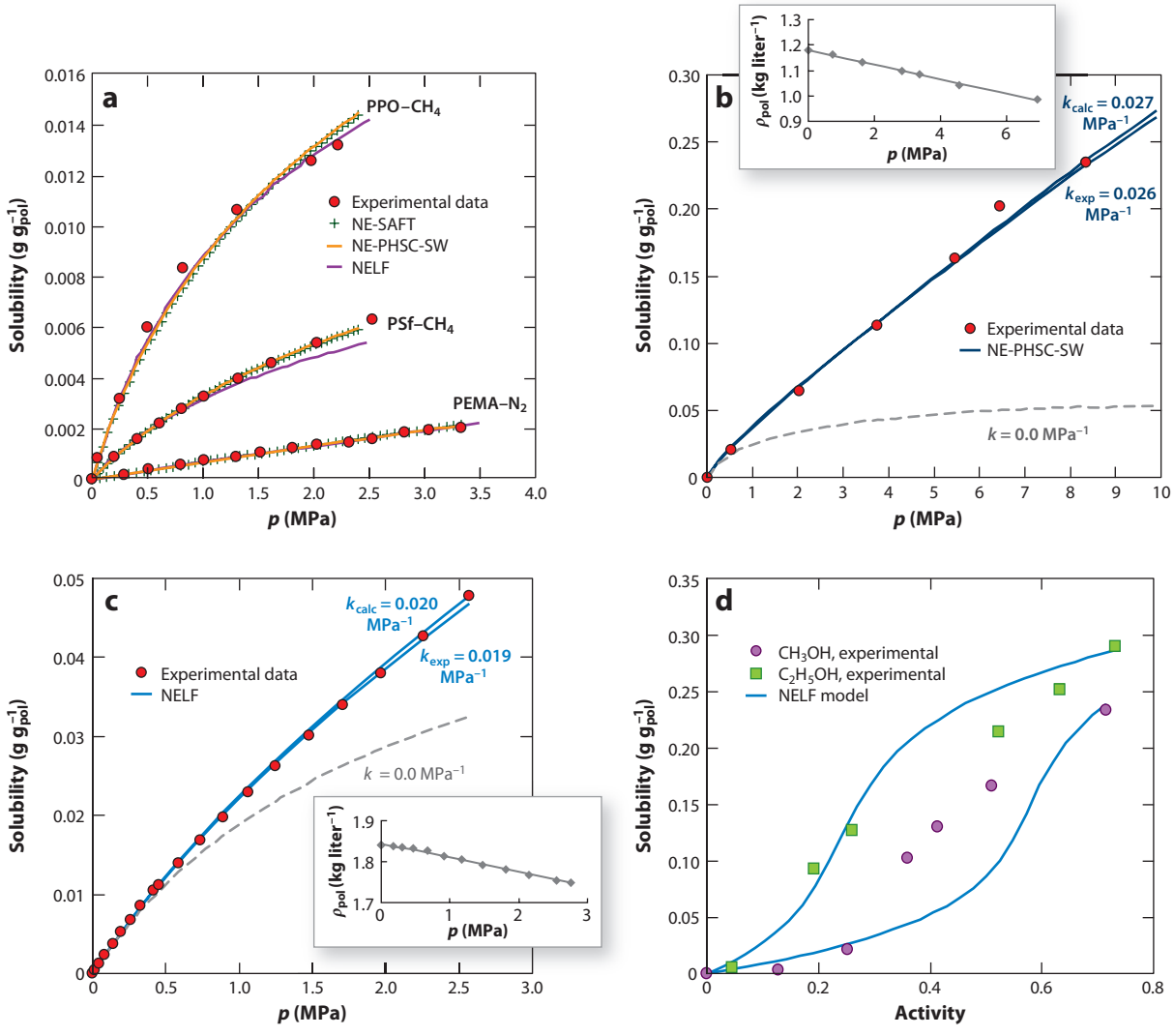

Figure 4

(*a*) Experimental sorption isotherms for the systems poly(phenylene oxide) (PPO)-CH_4, polysulfone (PSf)-CH_4, and poly(ethyl methacrylate) (PEMA)-N_2; the calculations of different nonequilibrium (NE) models [NE lattice fluid (NELF), NE-statistical associating fluid theory (SAFT), and NE-perturbed hard sphere chain-square well (NE-PHSC-SW)] are also shown (adapted from 47). (*b*) CO_2 solubility in poly(methyl methacrylate) (PMMA) at 33°C; the corresponding polymer dilation isotherms are reported as a function of pressure. The results of the NE-PHSC-SW model are reported for different values of the swelling coefficient (adapted from 47). (*c*) CO_2 solubility in Teflon® AF1600 at 35°C; the corresponding polymer dilation isotherms are reported as a function of pressure. The results of the NELF model are reported for different values of the swelling coefficient (adapted from 47). (*d*) Solubility of CH_3OH and C_2H_5OH in poly[1-(trimethylsilyl)-1-propyne] (PTMSP) at 25°C (71) and comparison with the NELF model predictions, with $k_{ij} = 0$ and $k_{sw} = 3\ MPa^{-1}$ for CH_3OH in PTMSP and $k_{sw} = 4\ MPa^{-1}$ for C_2H_5OH in PTMSP.

The solubility isotherms obtained from the nonequilibrium models for all of these systems are always satisfactory, and all models used give similar results. The worst case is represented by the PSf-CH_4 systems in which the NELF model slightly underestimates the experimental sorption data, especially at higher pressures; however, the error does not exceed 15% (47).

Solubility Isotherms of Swelling Gases and Vapors in Glassy Polymers

Application of NET-GP results to the solubility of swelling penetrants in glassy polymers is analyzed by considering the sorption of CO_2 in PMMA at 33°C (**Figure 4*b***) and in a perfluorinated matrix, Teflon® AF1600, at 35°C (**Figure 4*c***) (47). For both systems polymer dilation data are available from independent experimental measurements, and thus an experimental value of the swelling coefficient can be calculated. The swelling coefficient has also been estimated from the solubility data using the solubility model and a single, high-pressure solubility datum. As in the previous case, the model results obtained with a constant polymer density value have been included in **Figure 4*b*,*c*** and are represented by a dashed line. Based on these results, one can appreciate the importance of a correct estimation of volume dilation to account for the sorptive capacity of glassy polymers, especially at high pressure. The pure polymer density is 1.181 kg liter^{-1} for PMMA and 1.840 kg liter^{-1} for AF1600. The pure component characteristic parameters used in the calculation are reported in **Table 1**. From **Figure 4*b*,*c***, we conclude that the models used provide a good representation of the experimental data regardless of the procedure used to estimate the swelling coefficient and when using, at most, two experimental data points to retrieve the parameter values. In particular, the agreement is good between the value of the swelling coefficient obtained directly from the dilation data and that estimated from the model on the basis of one solubility datum: Such values are equal, respectively, to 0.026 and 0.027 MPa^{-1} for the CO_2-PMMA system and to 0.019 and 0.020 MPa^{-1} for the CO_2-AF1600 mixtures. For the CO_2-PMMA mixtures, k_{ij} was adjusted using a low-pressure solubility datum to obtain $k_{ij} = 0.075$, whereas for the CO_2-AF1600 mixture the default value $k_{ij} = 0.0$ was used (47).

In some hydrophobic, high free volume glassy polymers, the solubility isotherm of *n*-alkyl alcohol vapors is rather different from that of other gases and hydrocarbon vapors, as it has a sigmoidal shape with rather low values of mass uptake and positive concavity at low activity, followed by an inflection point after which the typical concavity of sorption in glassy polymers is recovered. This behavior was observed, for example, for methanol, ethanol, and propanol sorption in poly[1-(trimethylsilyl)-1-propyne] (PTMSP) (71–73) and PTMSN (74). In the most frequent cases, a positive concavity is observed in the rubbery phases at higher penetrant contents, whereas at lower penetrant activities, when the matrix is still a glass, downward concavity is typical. This unusual behavior is related to the unfavorable binary interactions between nonpolar polymers and polar solutes, which are more relevant at low penetrant content and attenuated by increasing the molecular weight of the *n*-alkyl alcohol, which leads to a stronger affinity between polymer and penetrant (71, 73). Interestingly, the S-shaped isotherms observed for alcohols cannot be explained, even qualitatively, by the DMS model (30), for which the sorption contribution of the excess free volume, C'_H, which is experimentally obtained by subtracting the Henry's law contribution from the actual isotherm, would be negative in the pressure range of the solubility isotherm that has positive concavity.

However, the qualitative difference observed between the solubility isotherms of alcohols and of other penetrants in PTMSP is an artifact associated with the representation of the solubility isotherms as penetrant concentration versus penetrant pressure. Indeed, by reporting the dimensionless, penetrant chemical potential $\ln(p/p_{ref})$ versus penetrant concentration, the qualitative

differences among the different penetrants vanish, and the effects of attractive or repulsive interactions between polymer and solutes become clearly apparent (72, 73).

The alcohol sorption behavior is well described by the NET-GP approach using the same procedure used for all other penetrants. The solubility isotherms of CH_3OH and C_2H_5OH in PTMSP at 25°C are plotted in **Figure 4*d*** (71). The density of pure PTMSP is 0.74 kg liter^{-1} (71). For the alcohols, the LF characteristic parameters were taken from previous studies, as were those for PTMSP, which were obtained by best fitting the S_0 value obtained from the NELF model (Equation 10) to a set of data for Ar, CO_2, H_2, N_2, O_2, CH_4, C_2H_6, C_3H_8, CF_4, C_2F_6, and C_3F_8 in PTMSP at 35°C (75), with $k_{ij} = 0.0$ and ρ_2^* fixed at 1.250 kg liter^{-1}, as suggested by previous studies including molecular simulations (76). All characteristic parameters are listed in **Table 1**.

One can thus use the NELF model to evaluate the solubility isotherms of CH_3OH and C_2H_5OH and then compare them with the experimental data. In such calculations, use has been made of $k_{ij} = 0.0$ for both penetrants, and k_{sw} in PTMSP was adjusted to 3 MPa^{-1} for CH_3OH and to 4 MPa^{-1} for C_2H_5OH. As **Figure 4*d*** shows, the NELF model qualitatively represents the sigmoidal shape of the solubility isotherm in both cases; for C_2H_5OH, the model also quantitatively represents with reasonable accuracy the experimental data.

Solubility of Liquids in Glassy Polymers

The NET-GP procedure is also applicable to liquid solutes. Examples are presented for water sorption in PC and PSf at different temperatures.

For the PC-water pair, the solubility isotherm from the vapor phase is available at 25°C (77). Application of the NELF model, using the pure component parameters reported in **Table 1**, gives a good representation of the observed behavior. The swelling coefficient is equal to zero, consistent with the rather limited solubilities, and $k_{ij} = 0.022$. Because Reference 77 does not report the densities of the glassy PC samples, we used the common pure glassy PC density value of 1.200 g cm^{-3}. The NELF model prediction can be calculated up to the pure liquid conditions using the same parameters and binary interaction parameter required to fit the low-pressure vapor solubility isotherm. Experimentally, the liquid water solubility is 0.0042 g g_{pol}^{-1} at 37.4°C (78). The PC density variation between 25°C and 37.4°C was considered negligible, and the pure polymer density was 1.200 g cm^{-3} for both cases. The same $k_{ij} = 0.022$ was used for the NELF prediction at both temperatures, and the model is able to represent both the solubility data from the vapor phase at 25°C and those from the liquid phase at 37.4°C, as shown in **Figure 5*a***.

By using the same model parameters as above, we can calculate in a completely predictive way the temperature dependence of the solubility of liquid water in PC from 25°C to 130°C and compare the results with the experimental data (79). To that aim, the variation with temperature of the pure polymer density is accounted for by using a volume thermal expansion coefficient of 19.5×10^{-5} K^{-1} (80). In the absence of a precise indication of the pure polymer density, we show in **Figure 5*b*,*c*** the results of NELF model calculations obtained by using for the pure polymer density at 25°C the values 1.20 and 1.21 g cm^{-3}, respectively, and $k_{ij} = 0.022$ (53). The NELF model offers a satisfactory estimation of the temperature dependence of the solubility of liquid water in PC in a rather broad temperature range.

Gas Solubility in Glassy Polymer Blends and Mixed-Gas Solubility in Glassy Polymers

More complex systems are frequently encountered in gas separations with polymeric membranes and in barrier polymer applications. The approach used above for binary mixtures also applies to polymer blends and mixed gases.

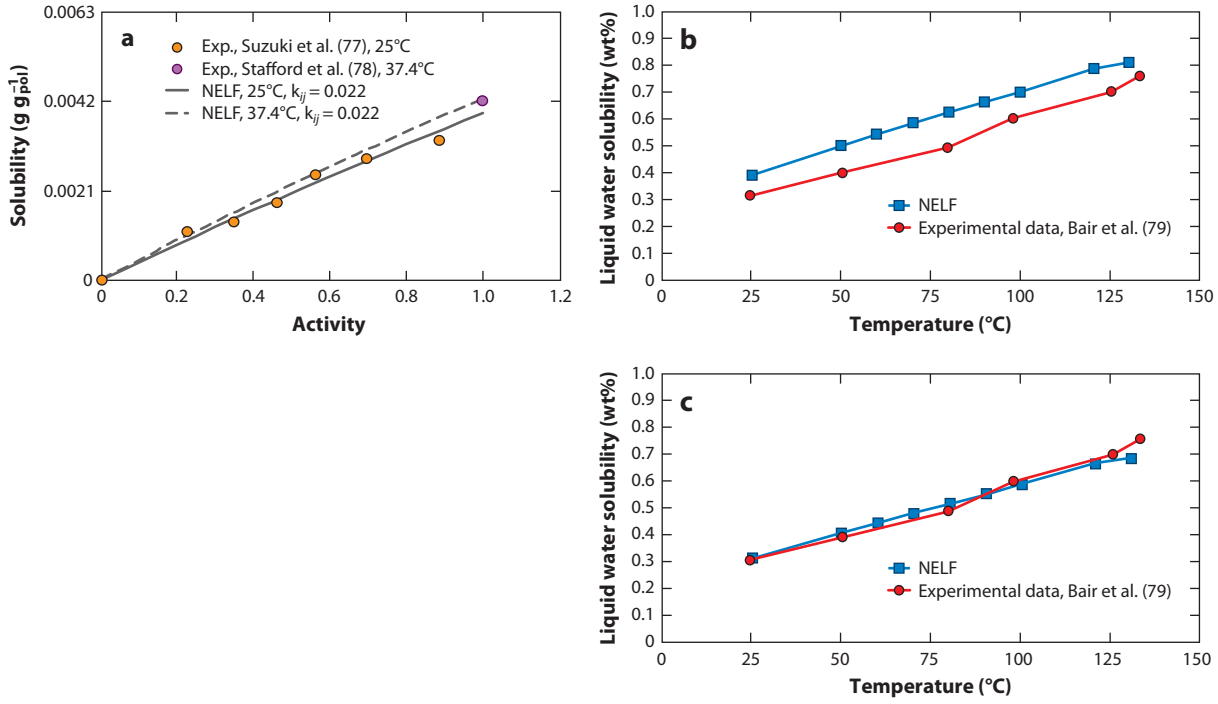

Figure 5

(*a*) Solubility of H_2O in polycarbonate (PC); orange circles indicate the vapor phase, purple circles indicate the liquid phase. Experimental data were taken at 25°C and 37.4°C (77, 78). (*b*,*c*) The solubility of liquid water in PC versus temperature, with a comparison between experimental data (79) and nonequilibrium lattice fluid (NELF) predictions with the pure polymer density at 25°C equal to 1.20 g cm^{-3} (*b*) and 1.21 g cm^{-3} (*c*). Figure adapted from Reference 53.

The solubility in two glassy polymer blends is reported in **Figure 6**, which shows the solubility isotherms of CH_4 in polystyrene-tetramethyl polycarbonate (PS-TMPC) blends of different compositions (0–20–40–60–100% PS) at 35°C (**Figure 6*a***), and the solubility isotherms of CO_2 in five blends of (bisphenol-chloral) polycarbonate (BCPC) and PMMA (0–25–50–75% PMMA) at 35°C (**Figure 6*b***) (47). The NELF estimation of the solubility is also reported on the basis of only the pure component characteristic parameters and the pure polymer sorption isotherm. This allows the calculation of the k_{ij} values for the systems considered, which are −0.010 and −0.059 for CH_4 in TMPC and PS, respectively, and −0.016 and −0.028 for CO_2 in BCPC and PMMA, respectively (47). In all cases $k_{ij} = 0.0$ was used for the polymer-polymer pairs. The pure component parameters used are reported in **Table 1**, whereas the parameters for the blends were calculated from those of the pure homopolymers through the model mixing rules (81). The swelling coefficient of the blend is calculated as the volumetric average of the pure polymer swelling coefficients, on the basis of the volume fractions in the unpenetrated blends (81). Using the swelling and binary interaction parameters obtained from the sorption isotherms in pure polymers means that calculation of solubility in the blends is entirely predictive, and agreement with the experimental data is quite good. Thus, the model accurately predicts the solubility isotherms of the glassy blends when the pure polymer sorption isotherm for the solvent under investigation is known. The results are more than satisfactory, with average errors that seldom exceed 10% for PS-TMPC blends and are generally lower for the other blends considered.

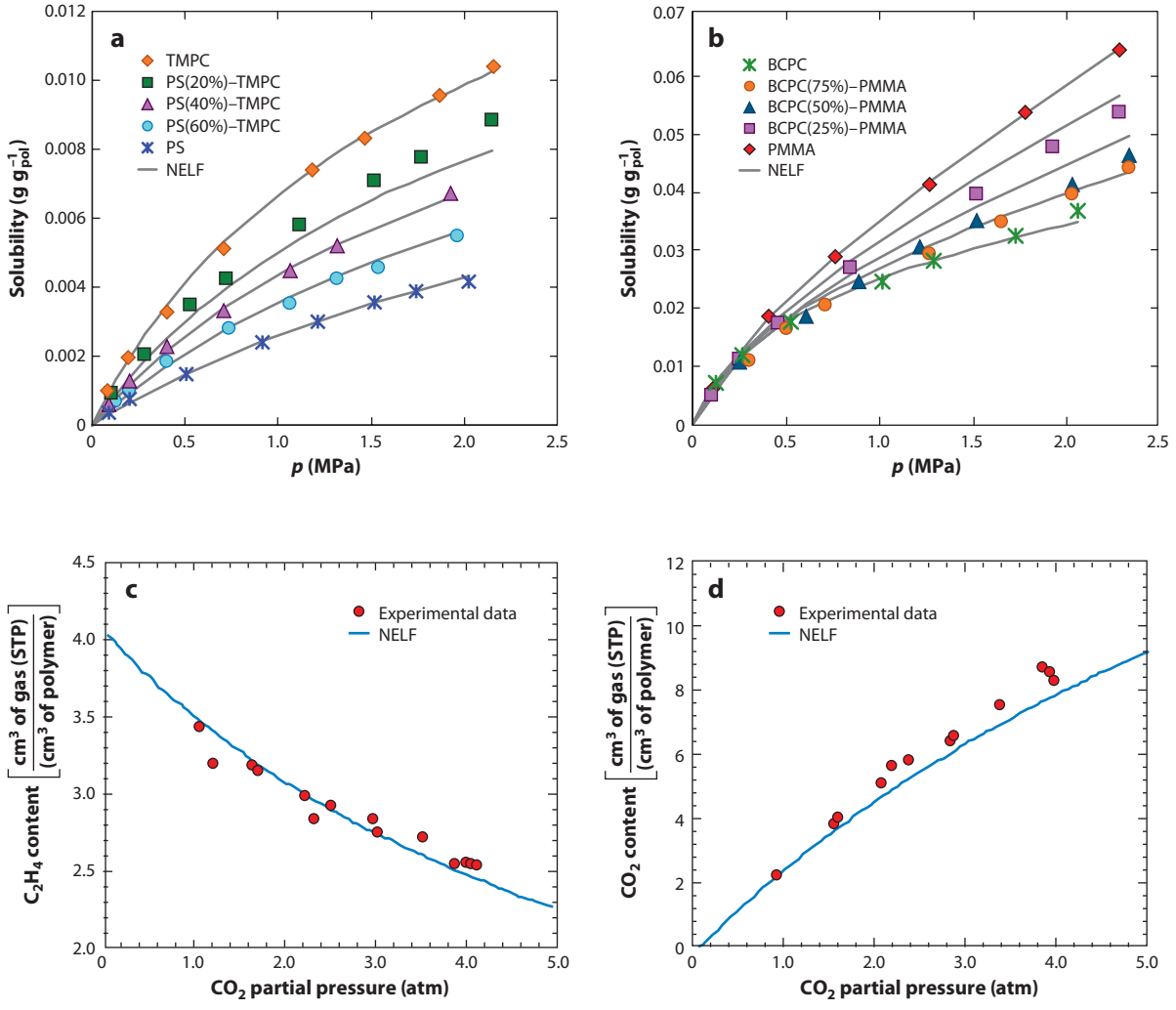

Figure 6

(*a*) Experimental CH_4 solubility in polystyrene-tetramethyl polycarbonate (PS-TMPC) blends and (*b*) CO_2 solubility in BCPC-PMMA [(bisphenol-chloral) polycarbonate–poly(methyl methacrylate)] blends at 35°C as well as nonequilibrium lattice fluid (NELF) model results for both systems. Experimental (*c*) C_2H_4 and (*d*) CO_2 concentrations in a ternary PMMA-C_2H_4-CO_2 mixture as a function of CO_2 partial pressure, with constant C_2H_4 fugacity in the vapor phase. The solid line represents the NELF prediction based on the binary mixture data. STP, standard temperature and pressure. Figure adapted from Reference 47.

The same procedure applies to mixed gas sorption in a single glassy polymer, for example, the system PMMA-CO_2-C_2H_4 at 35°C (50); **Figure 6*c,d*** compares experimental and NELF model predictions for this system (47). In this case, the binary interaction parameters for both polymer-penetrant pairs were set to the default values ($k_{12} = k_{13} = 0.0$), and swelling was neglected in view of the relatively low pressure range inspected. Vapor-liquid equilibrium data for the penetrant mixture were used for the evaluation of the C_2H_4-CO_2 binary interaction parameter to obtain $k_{23} = 0.024$. Therefore, extension of NELF to the ternary system does not require any additional adjustable parameters, and the model is completely predictive (47). In **Figure 6*c,d***, CO_2 and C_2H_4

concentrations in the polymer are reported as a function of CO_2 partial pressure in the external gaseous phase when the ethylene partial pressure is held constant at 2.06 ± 0.08 atm.

For the mixed gases considered, the nonequilibrium model predicts the experimental data quite well; the ethylene content is well calculated, and the slight underestimation of the CO_2 content at the higher penetrant partial pressure can be attributed to polymer swelling that probably occurs in such conditions and has been neglected in the calculation.

Gas Solubility in Mixed Matrix Membranes Based on Glassy Polymers

In the field of membranes for gas separation, great attention has been paid to nanocomposite glassy phases in view of their unusual and interesting behavior; indeed, the performance of membranes composed of polymer materials can be improved by the addition of inorganic fillers. The NET-GP model is useful to evaluate the sorption and transport properties of gases and vapors in mixed matrix membranes, whose characterization would otherwise require extensive experimental work.

In particular, the systems examined in detail are the nanocomposites formed by adding hydrophobic, impermeable fumed silica (FS) nanoparticles to high free volume glassy polymers such as PTMSP and amorphous Teflon® AF. These nanocomposite materials exhibit a general and significant enhancement of gas solubility, diffusivity, and permeability with respect to the unloaded polymers, whereas the effects on gas selectivity may be different from each other (82). Despite numerous experimental studies, the interpretation of mixed matrix behavior is not reached through traditional procedures, as solubility is not additive in these composites and permeability does not obey classical theories for composites such as the Maxwell model (83).

Both positron annihilation lifetime spectroscopy (PALS) and density measurements have indicated that such matrices have higher FFV with respect to the pure unloaded glassy polymeric phase (82). However, those measurements are often not accurate enough to estimate the FFV variation induced by the addition of filler in the polymer.

The NET-GP procedure is a successful method for estimating the accessible free volume variation in such materials (84). It assumes that the density and sorption capacity of the solid filler remain unchanged upon mixing, whereas the polymer density changes, which causes the observed variation in sorption and transport properties. That reasonable assumption requires the use of a single parameter to describe the composite behavior, namely the polymer density, and does not invoke the presence of a third interfacial region with distinct properties.

The procedure used estimates the polymer density variation owing to filler loading from the experimental sorption data of one, nonswelling test gas (TG) (e.g., CH_4) in the filler, $C^0_{TG,F}$ (should it not be negligible, as it is frequently), and in composite matrix, $C_{TG,M}$, with filler volume fraction Φ_F. By assuming that the filler sorption capacity does not change upon mixing with the polymer, one obtains the sorption in the polymeric phase of the composite, $C_{TG,P}$, as (84):

$$C_{TG,P} = \frac{C_{TG,M} - \Phi_F C^0_{TG,F}}{(1 - \Phi_F)}. \qquad 14.$$

This quantity is then used in the NELF model, which relates the sorption capacity in the glassy polymer to the pure polymer density, ρ^0_{pol}. Calculation of ρ^0_{pol} for the polymer phase allows us to estimate the FFV of the polymer in the mixed matrix state, FFV^0_M, with respect to the occupied volume as usual,

$$FFV^0_M = \frac{\rho^{vdW}_{pol} - 1.3\rho^0_{pol}}{\rho^{vdW}_{pol}}, \qquad 15.$$

where ρ_{pol}^{vdW} is the van der Waals density of the polymer, which is available from the literature. In the above expression the occupied volume is considered equal to 1.3 times the van der Waals volume (85).

The FFV values thus calculated for each filler are then used to estimate a priori the solubility of other gases in the various composite materials using the same NELF model. For swelling penetrants one also has to fit the swelling parameter, k_{sw}.

The FFV value can also be used to estimate, with two adjustable parameters A and B, the infinite dilution diffusivity of gases in mixed matrix membranes by means of calculation based on free volume theory (84),

$$D_{i,M}^{0} = \frac{1}{\tau} \exp\left(A - \frac{B}{FFV_{M}^{0}}\right), \qquad 16.$$

where the tortuosity, τ, is given by $\tau = 1 + \frac{\Phi_F}{2}$ as per Maxwell's model (83).

As an example, we review mixed matrices based on amorphous Teflon® AF1600 and AF2400 and variable amounts of FS. To evaluate the FFV variation of the polymeric phase induced by filler addition, the polymer density in the mixed matrix state was estimated by fitting the NELF model to the solubility isotherms of CH_4, a nonswelling penetrant suitable as a test probe. The densities of the polymer phase calculated from methane sorption data decrease with increasing FS content, as expected: in particular they have the values 1.740 kg liter^{-1} for pure AF2400, 1.714 kg liter^{-1} for AF2400 with 25 wt% of FS, and 1.690 kg liter^{-1} for AF2400 with 40 wt% FS. Similar behavior is observed for AF1600-based mixed matrices (84).

Moreover, the density values estimated with the NELF model can be used to predict the solubility of all the other penetrants examined (CO_2, n-C_4, n-C_5) in the same mixed matrices, as shown in **Figure 7** for AF2400-based materials. To describe the sorption isotherms of these penetrants over the entire pressure range examined, one needs to adjust another parameter, k_{sw}, to the experimental high pressure solubility data of each penetrant. Indeed, k_{sw} is not merely an empirical fitting parameter because it has a precise physical meaning and represents the extent of swelling induced by each penetrant, as shown by comparing the calculated and experimental values for n-butane and n-pentane sorption-induced dilation. The k_{sw} values obtained experimentally for n-C_4 in AF2400-based matrices are 0.34, 0.49, and 0.97 MPa^{-1} for AF2400, AF2400-25FS, and AF2400-40FS, respectively, similar to those obtained by modeling sorption isotherms with NELF (i.e., 0.40, 0.40, and 0.48 MPa^{-1} for the three matrices). Swelling coefficients of n-C_5 in AF2400-based mixed matrices increase from 0.68 to 0.98 to 1.35 MPa^{-1} for AF2400, AF2400-25FS, and AF2400-40FS, respectively; these values are qualitatively consistent with those obtained with the NELF model (0.91, 1.23, and 1.99 MPa^{-1}). Similar agreement is observed for the swelling coefficients of n-C_4 sorption in AF1600- and AF2400-based mixed matrices. Use of the experimentally obtained k_{sw} in place of the adjusted ones yields a maximum deviation from the actual solubility value of approximately −20% in AF2400-based matrices (84).

As shown in **Figure 8*a*** for the diffusion of n-pentane in both AF2400 and AF1600, there is a strong correlation between $D_M^0\tau$ and 1/FFV, as expected from Equation 16. Furthermore, the same exponential correlation can be used for mixed matrix membranes based on both Teflon® AF1600 and AF2400. That behavior likely occurs because both polymeric matrices have the same chemical structure; the main difference between them is the amount of free volume present in the matrix, which is the key parameter governing penetrant diffusion. Similar behavior is observed for n-butane diffusion (84).

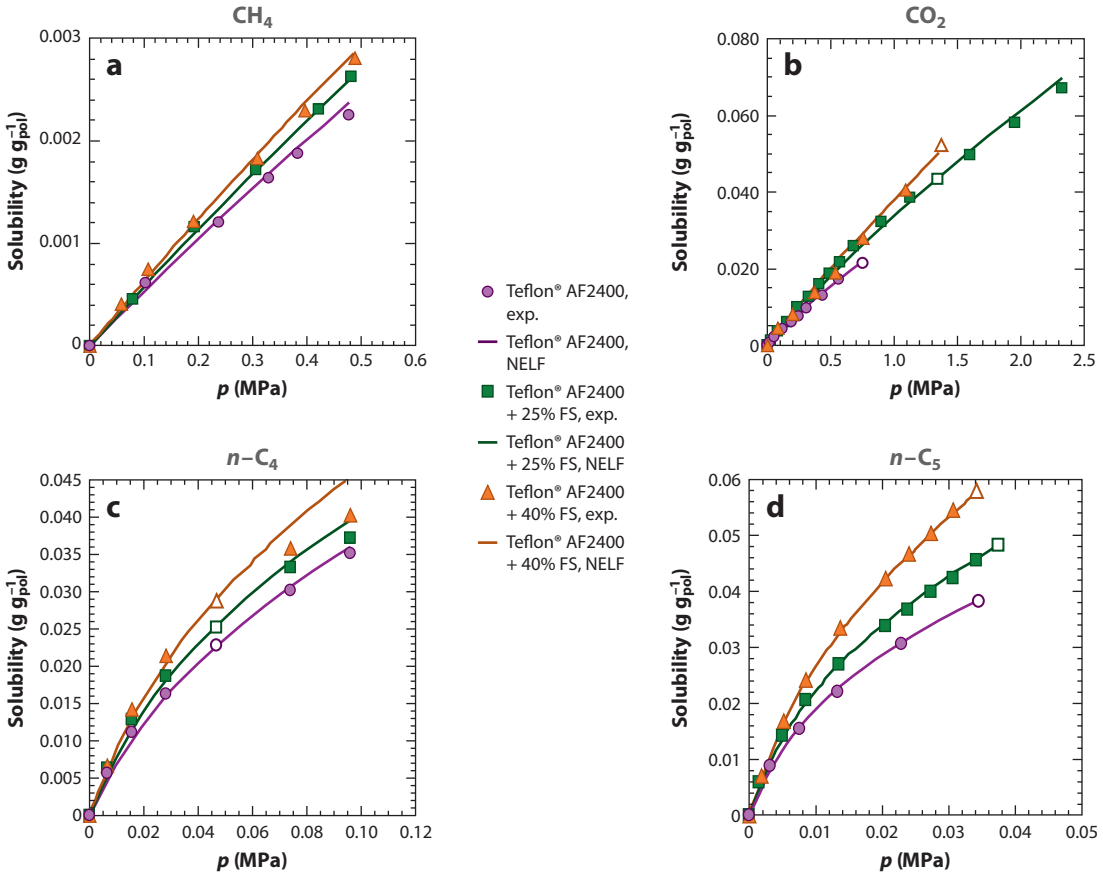

Figure 7

Experimental solubility of (*a*) CH_4 and (*b*) CO_2 at 35°C as well as (*c*) *n*-C_4 and (*d*) *n*-C_5 at 25°C in the polymeric phase of amorphous Teflon® AF2400-based mixed matrix membranes containing fumed silica (FS) and comparisons with nonequilibrium lattice fluid (NELF) model calculations. Open symbols indicate the solubility data points used to estimate k_{sw}. Figure adapted from Reference 84.

Finally, by considering the dependence of the diffusion coefficient on the penetrant concentration, which is well represented by the equation

$$D_{i,M} = D^0_{i,M} \exp(\beta C_{i,P}), \qquad 17.$$

the behavior of the adjustable coefficient β, which represents the dependence of diffusivity on the concentration in the polymer phase, was also studied. In most polymer-penetrant systems, the vapor diffusivity increases with penetrant concentration, especially for swelling penetrants and for polymers characterized by moderate FFV values. This behavior occurs because diffusive jumps of penetrants in polymers become more frequent if the presence of a penetrant plasticizes the matrix. Also, the penetrant-induced swelling increases the FFV available for diffusion. Interestingly, the β values for the materials examined in this work are also related to the FFV obtained from the solubility data of CH_4 (**Figure 8*b***) through an exponential law (84),

$$\beta = E \cdot \exp(-F \cdot FFV^0_M). \qquad 18.$$

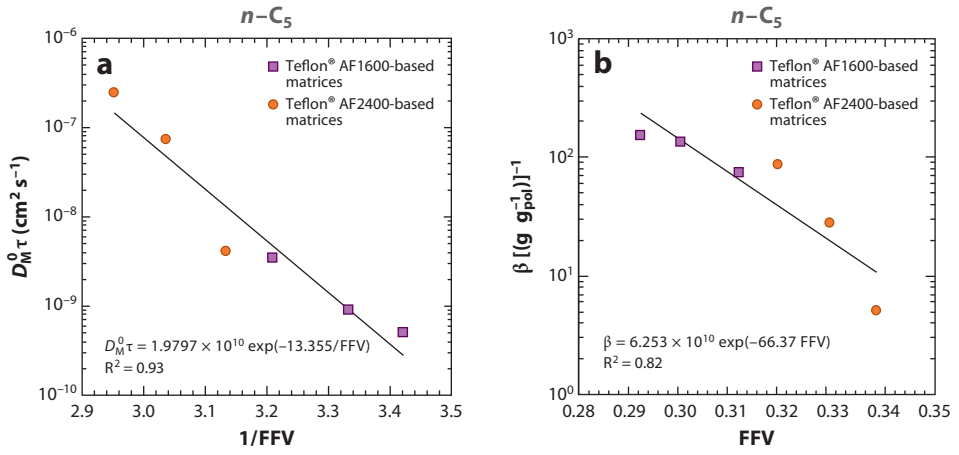

Figure 8

(*a*) Infinite dilution diffusion coefficient of *n*-C_5 in the polymeric phase of mixed matrices based on Teflon® AF2400 and AF1600 as a function of reciprocal fractional free volume (1/FFV). (*b*) β coefficient for diffusion of *n*-C_5 in mixed matrices based on AF2400 and AF1600 as a function of FFV. Figure adapted from Reference 84.

The above correlation is rather novel and implies that the higher the initial FFV in the matrix, the lower the value of β, i.e., the less important the effect of penetrant concentration on diffusion. Furthermore, a single master curve can be drawn for both AF1600 and AF2400, and the parameters *E* and *F* are both positive and depend, reasonably, on the penetrant type (84).

That behavior can be explained by the fact that if the initial free volume is larger, the diffusivity is already relatively high, and consequently its dependency on FFV variations induced by swelling is lower. Therefore, the diffusion-enhancing effect that accompanies an increase in penetrant concentration, through swelling and plasticization, is lower for matrices with higher FFV. The above correlation also implies that β decreases with increasing silica content in the matrix. Although apparently this behavior could be explained by silica-induced rigidification of the polymeric matrices, the direct swelling data shown above do not confirm this explanation, at least in the case of AF2400, because the measured volume dilation does not decrease with increasing silica content. Silica loading mainly increases the free volume of the polymer, rather than affects its rigidity, as is consistent with the observed independence from silica content of T_g, which is a measure of the chain mobility (84).

CONCLUSIONS

The solubility of low-molecular-weight solutes in glassy polymeric phases can be satisfactorily calculated via proper use of EoS models such as LF, SAFT, and PHSC if they are suitably adapted via NET-GP for the nonequilibrium conditions into the corresponding NELF, NE-SAFT, and NE-PHSC models. For all isotropic phases including single polymers as well as polymer blends, the actual polymer density is the only nonequilibrium property that is required to account for the departure from equilibrium frozen into the glass. The pure-component parameters of the models can be obtained from independent information, and the only other parameters needed are the binary interaction parameter for each pair of chemical species and, for swelling solutes, the swelling coefficient of each swelling penetrant. In many ways, the procedure followed is parallel

to the one using an EoS in the calculation of usual fluid-phase equilibria, with the difference that the nonequilibrium density of the polymer must be used.

As for the traditional application of an EoS, in general this approach requires a more limited number of adjustable parameters and in many cases is entirely predictive using pure component parameters and the default value of the binary interaction parameter. The predictive ability of the model has been shown in several cases for the solubility isotherms of nonswelling solutes in pure polymers as well as, more importantly, for the solubility isotherms of polymer blends or mixed gases, using binary parameters for all the pairs formed by the species present in the multicomponent mixture.

DISCLOSURE STATEMENT

The authors are not aware of any affiliations, memberships, funding, or financial holdings that might be perceived as affecting the objectivity of this review.

LITERATURE CITED

1. Fleming GK, Koros WJ. 1990. Carbon dioxide conditioning effects on sorption and volume dilation behavior for bis-phenol-A-polycarbonate. *Macromolecules* 23:1353–60
2. Enscore DJ, Hopfenberg HB, Stannett VT. 1980. Diffusion, swelling, and consolidation in glassy polystyrene microspheres. *Polym. Eng. Sci.* 20:102–7
3. Sarti GC, Gostoli C, Masoni S. 1983. Diffusion of alcohols and relaxation in poly(methyl methacrylate): effect of thermal history. *J. Membr. Sci.* 15:181–92
4. Pope DS, Koros WJ. 1992. Effect of various preexposure agents on methane sorption and dilation in tetramethyl polycarbonate. *Macromolecules* 25:1711–15
5. Flory PJ. 1941. Thermodynamics of high polymer solutions. *J. Chem. Phys.* 9:660–61
6. Huggins ML. 1941. Solutions of long chain compounds. *J. Chem. Phys.* 9:440
7. Abrams DS, Prausnitz JM. 1975. Statistical thermodynamics of liquid mixtures: a new expression for the Gibbs energy of partly or completely miscible systems. *AIChE J.* 21:116–28
8. Oishi T, Prausnitz JM. 1978. Estimation of solvent activities in polymer solutions using a group-contribution method. *Ind. Eng. Chem. Res.* 17:333–39
9. Elbro HS, Fredenslund A, Rasmussen P. 1990. New simple equation for the prediction of solvent activities in polymer solutions. *Macromolecules* 23:4707–14
10. Patterson D. 1969. Free volume and polymer solubility. A qualitative view. *Macromolecules* 2:672–77
11. Flory PJ. 1970. Thermodynamics of polymer solutions. *Discuss. Faraday Soc.* 49:7–29
12. Sanchez IC, Lacombe RH. 1978. Statistical thermodynamics of polymer solutions. *Macromolecules* 11:1145–56
13. Huang SH, Radosz M. 1990. Equation of state for small, large, polydisperse, and associating molecules. *Ind. Eng. Chem. Res.* 29:2284–94
14. Song Y, Hino T, Lambert SM, Prausnitz JM. 1996. Liquid-liquid equilibria for polymer solutions and blends, including copolymers. *Fluid Phase Equilib.* 117:69–76
15. Hino T, Prausnitz JM. 1997. Perturbed hard-sphere-chain equation of state for normal fluids and polymers using the square-well potential of variable width. *Fluid Phase Equilib.* 138:105–30
16. Kang JW, Lee JH, Yoo KP, Lee CS. 2002. Extended hydrogen-bonding lattice fluid theory for dimers and n-mers. *Fluid Phase Equilib.* 194:77–86
17. Doghieri F, Quinzi M, Rethwisch DG, Sarti GC. 2006. Predicting gas solubility in glassy polymers through non-equilibrium EOS. In *Materials Science of Membranes for Gas and Vapor Separation*, ed. Y Yampolskii, I Pinnau, BD Freeman, 1:137–58. New York: Wiley
18. Theodorou DN. 2006. Principles of molecular simulation of gas transport in polymers in material science of membranes. In *Materials Science of Membranes for Gas and Vapor Separation*, ed. Y Yampolskii, I Pinnau, BD Freeman, pp. 1:47–92. New York: Wiley

19. Allen MP, Tildesley DJ. 1987. *Computer Simulation of Liquids*. Oxford: Clarendon. 412 pp.
20. Panagiotopoulos AZ, Suter UW, Reid RC. 1986. Phase diagrams of nonideal fluid mixtures from Monte Carlo simulation. *Ind. Eng. Chem. Fundam.* 25:525–35
21. Widom BJ. 1963. Some topics in the theory of fluids. *Chem. Phys.* 39:2808–12
22. Boulougouris GC, Economou IG, Theodorou DN. 1999. On the calculation of the chemical potential using the particle deletion scheme. *Mol. Phys.* 96:905–13
23. Siegert MR, Heuchel M, Hofmann DJ. 2007. A generalized direct-particle-deletion scheme for the calculation of chemical potential and solubilities of small- and medium-sized molecules in amorphous polymers. *Comput. Chem.* 28:877–89
24. Spyriouni T, Boulougouris GC, Theodorou DN. 2009. Prediction of sorption of CO_2 in glassy atactic polystyrene at elevated pressures through a new computational scheme. *Macromolecules* 42:1759–69
25. De Angelis MG, Boulougouris GC, Theodorou DN. 2010. Prediction of infinite dilution benzene solubility in linear polyethylene melts via the direct particle deletion method. *J. Phys. Chem. B* 114:6233–46
26. Theodorou DN, Suter UW. 1985. Detailed molecular structure of a vinyl polymer glass. *Macromolecules* 18:1467–78
27. Heuchel M, Bohning M, Holck O, Siegert MR, Hofmann D. 2006. Atomistic packing models for experimentally investigated swelling states induced by CO_2 in glassy polysulfone and poly(ether sulfone). *J. Polym. Sci. Part B* 44:1874–97
28. Van Der Vegt NFA, Briels WJ, Wessling M, Strathmann H. 1999. Sorption induced glass transition in amorphous glassy polymers. *J. Chem. Phys.* 110:11061–69
29. Kanellopoulos V, Mouratides D, Pladis P, Kiparissides C. 2006. Prediction of solubility of α-olefins in polyolefins using a combined equation of state–molecular dynamics approach. *Ind. Eng. Chem. Res.* 45:5870–78
30. Barrer RM, Barrie JA, Slater J. 1958. Sorption and diffusion in ethyl cellulose. Part III. Comparison between ethyl cellulose and rubber. *J. Polym. Sci.* 27:177–97
31. Michaels AS, Vieth WR, Barrie JA. 1963. Solution of gases in polyethylene terephthalate. *J. Appl. Phys.* 34:1–12
32. Jordan SS, Koros WJ. 1995. A free volume distribution model of gas sorption and dilation in glassy polymers. *Macromolecules* 28:2228–35
33. Fleming GK, Koros WJ. 1986. Dilation of polymers by sorption of carbon dioxide at elevated pressures. 1. Silicone rubber and unconditioned polycarbonate. *Macromolecules* 19:2285–91
34. Bondar VI, Kamiya Y, Yampol'skii YP. 1996. On pressure dependence of the parameters of the dual-mode sorption model. *J. Polym. Sci. Part B* 34:369–78
35. Conforti RM, Barbari TA, Vimalchand P, Donohue MD. 1991. Lattice-based activity coefficient model for gas sorption in glassy polymers. *Macromolecules* 24:3388–94
36. Wissinger RG, Paulaitis ME. 1991. Molecular thermodynamic model for sorption and swelling in glassy polymer-CO_2 systems at elevated pressures. *Ind. Eng. Chem. Res.* 30:842–51
37. Mi Y, Zhou S, Stern SA. 1991. Representation of gas solubility in glassy polymers by a concentration-temperature superposition principle. *Macromolecules* 24:2361–67
38. Vrentas JS, Vrentas CM. 1991. Sorption in glassy polymers. *Macromolecules* 24:2404–12
39. Lipscomb GG. 1990. Unified thermodynamic analysis of sorption in rubbery and glassy materials. *AIChE J.* 36:1505–16
40. Coleman BD, Gurtin ME. 1967. Thermodynamics with internal state variables. *J. Chem. Phys.* 47:597–613
41. Sanchez IC, Lacombe RH. 1976. An elementary molecular theory of classical fluids. Pure fluids. *J. Phys. Chem.* 80:2352–62
42. Lacombe RH, Sanchez IC. 1976. Statistical thermodynamics of fluid mixtures. *J. Phys. Chem.* 80:2568–80
43. Chapman WG, Gubbins KE, Jackson G, Radosz M. 1989. SAFT. Equation-of-state solution model for associating fluids. *Fluid Phase Equilib.* 52:31–38
44. Chapman WG, Gubbins KE, Jackson G, Radosz M. 1990. New reference equation of state for associating liquids. *Ind. Eng. Chem. Res.* 29:1709–21
45. Song Y, Lambert SM, Prausnitz JM. 1994. Equation of state for mixtures of hard-sphere chains including copolymers. *Macromolecules* 27:441–48

46. Doghieri F, Sarti GC. 1996. Nonequilibrium lattice fluids: a predictive model for the solubility in glassy polymers. *Macromolecules* 29:7885–96
47. Giacinti Baschetti M, De Angelis MG, Doghieri F, Sarti GC. 2005. Solubility of gases in polymeric membranes. In *Chemical Engineering: Trends and Developments*, ed. MA Galan, E Martin del Valle, 1:41–61. Chichester, UK: Wiley
48. Doghieri F, De Angelis MG, Giacinti Baschetti M, Sarti GC. 2006. Solubility of gases and vapors in glassy polymers modelled through non-equilibrium PHSC theory. *Fluid Phase Equilib.* 241:300–7
49. Wissinger G, Paulaitis ME. 1987. Swelling and sorption in polymer-CO_2 mixtures at elevated pressures. *J. Polym. Sci. Part B* 25:2497–510
50. Giacinti Baschetti M, Doghieri F, Sarti GC. 2001. Solubility in glassy polymers: correlations through the nonequilibrium lattice fluid model. *Ind. Eng. Chem. Res.* 40:3027–37
51. De Angelis MG, Doghieri F, Sarti GC. 2007. NELF model prediction of the infinite dilution gGas solubility in glassy polymers. *J. Membr. Sci.* 289:106–22
52. De Angelis MG, Sarti GC, Doghieri F. 2007. Correlations between penetrant properties and infinite dilution gas solubility in glassy polymers: NELF model derivation. *Ind. Eng. Chem. Res.* 46:7645–56
53. Sarti GC, De Angelis MG. 2010. Calculation of the solubility of liquid solutes in glassy polymers. *AIChE J.* In press
54. Zoller P, Walsh D. 1995. *Standard Pressure-Volume-Temperature Data for Polymers*. Lancaster, PA: Technomic
55. Finkelshtein E, Makovetskii KL, Gringolts M, Rogan YV, Golenko TG, et al. 2006. Addition-type polynorbornenes with $Si(CH_3)_3$ side groups: synthesis, gas permeability, and free volume. *Macromolecules* 39:7022–29
56. Starannikova L, Pilipenko M, Belov N, Yampolskii Y, Gringolts M, Finkelshtein E. 2008. Addition-type polynorbornene with $Si(CH_3)_3$ side groups: detailed study of gas permeation and thermodynamic properties. *J. Membr. Sci.* 323:134–43
57. Galizia M, De Angelis MG, Sarti GC. 2009. Characterization and modeling of the organic vapour transport in addition-type poly (trimethylsilyl norbornene). *AIDIC Conf. Ser.* 9:139–48
58. Prabhakar RS, De Angelis MG, Sarti GC, Freeman BD, Coughlin MC. 2005. Gas and vapor sorption, permeation, and diffusion in poly(tetrafluoroethylene-co-perfluoromethyl vinyl ether). *Macromolecules* 38:7043–55
59. De Angelis MG, Merkel TC, Bondar VI, Freeman BD, Doghieri F, Sarti GC. 2002. Gas sorption and dilation in poly(2,2-bistrifluoromethyl-4,5-difluoro-1,3-dioxole-*co*-tetrafluoroethylene): comparison of experimental data with predictions of the nonequilibrium lattice fluid model. *Macromolecules* 35:1276–88
60. De Angelis MG, Merkel TC, Bondar VI, Freeman BD, Doghieri F, Sarti GC. 1999. Hydrocarbon and fluorocarbon solubility and dilation in poly(dimethylsiloxane): comparison of experimental data with predictions of the Sanchez-Lacombe equation of state. *J. Polym. Sci. Part B* 37:3011–26
61. van Amerongen GJ. 1950. Influence of structure of elastomers on their permeability to gases. *J. Polym. Sci.* 5:307–32
62. Barrer RM, Skirrow G. 1948. Transport and equilibrium phenomena in gas-elastomer systems. *J. Polym. Sci.* 3:564–75
63. Korosy F. 1937. Two rules concerning solubility of gases and crude data on solubility of krypton. *Trans. Faraday Soc.* 33:416–25
64. Michaels AS, Bixler HJ. 1961. Solubility of gases in polyethylene. *J. Polym. Sci.* 50:393–412
65. Kamiya Y, Naito Y, Terada K, Mizoguchi K. 2000. Volumetric properties and interaction parameters of dissolved gases in poly(dimethylsiloxane) and polyethylene. *Macromolecules* 33:3111–19
66. Ghosal K, Chern RY, Freeman BD, Savariar RJ. 1995. The effect of aryl nitration on gas sorption and permeation in polysulfone. *J. Polym. Sci. Part B* 33:657–66
67. Toi K, Morel G, Paul DR. 1981. Gas sorption and transport in poly-(phenylene oxide) and comparisons with other glassy polymers. *J. Appl. Polym. Sci.* 27:2997–3005
68. Serad GE, Freeman BD, Stewart ME, Hill AJ. 2001. Gas and vapor sorption and diffusion in poly(ethylene terephthalate). *Polymer* 42:6929–43
69. Gee G. 1947. Some thermodynamic properties of high polymers and their molecular interpretation. *Q. Rev.* (*Lond.*) 1:265–98

70. Chiou JS, Paul DR. 1989. Gas sorption and permeation in poly(ethyl methacrylate). *J. Membr. Sci.* 45:167–89
71. Nakanishi K, Odani H, Kurata M, Masuda T, Higashimura T. 1987. Sorption of alcohol vapors in a disubstituted polyacetilene. *Polym. J.* 19:293–304
72. Doghieri F, Biavati D, Sarti GC. 1996. Solubility and diffusivity of ethanol in PTMSP: effects of activity and of polymer aging. *Ind. Eng. Chem. Res.* 35:2420–30
73. Doghieri F, Giacinti Baschetti M, Nicolini L, Sarti GC. 1999. Sorption and diffusion of *n*-alkanes and alcohols in poly(1-trimethylsilyl-1-propyne). *ACS Symp. Ser.* 733:38–55
74. Galizia M. 2010. *Trasporto di materia in membrane polimeriche e nanocomposite per la separazione di gas*. PhD thesis. Università di Bologna. 220 pp.
75. Srinivasan R, Auvil SR, Burban PM. Elucidating the mechanism(s) of gas transport in poly[1-(trimethylsilyl)-1-propyne] (PTMSP) membranes. *J. Membr. Sci.* 86:67–86
76. Giacinti Baschetti M, Ghisellini M, Quinzi M, Doghieri F, Stagnaro P, et al. 2005. Effects on sorption and diffusion in PTMSP and TMSP/TMSE copolymers of free volume changes due to polymer ageing. *J. Mol. Struct.* 739:75–86
77. Suzuki T, Chihara H, Kotaka T. 1984. Sorption of water by bisphenol-A polycarbonate and polyoxyethylene multiblock copolymers with varying composition and block length. *Polym. J.* 16:129–38
78. Stafford GD, Braden M. 1968. Water absorption of some denture base polymers. *J. Dent. Res.* 47:341
79. Bair HE, Johnson GE, Merriweather R. 1978. Water sorption of polycarbonate and its effect on the polymer's dielectric behavior. *J. Appl. Phys.* 49:4976–84
80. Engineer's Handbook. 2006. *Plastic thermal expansion coefficients*. **http://www.engineershandbook.com/Tables/plasticthermalexp.htm**
81. Grassia F, Giacinti Baschetti M, Doghieri F, Sarti GC. 2004. Solubility of gases and vapors in glassy polymer blends. In *Advanced Materials for Membrane Separations*, ed. I Pinnau, BD Freeman, 1:55–73. New York: Oxford Univ. Press
82. Merkel TC, Freeman BD, Spontak RJ, He Z, Pinnau I, et al. 2002. Ultrapermeable, reverse-selective nanocomposite membranes. *Science* 296:519–22
83. Maxwell C. 1873. *Treatise on Electricity and Magnetism*. London: Oxford Univ. Press. 484 pp.
84. Ferrari MC, Galizia M, De Angelis MG, Sarti GC. 2010. Gas and vapor transport in mixed matrix membranes based on amorphous Teflon AF1600 and AF2400 and fumed silica. *Ind. Eng. Chem. Res.* 49:11920–35
85. van Krevelen W. 1990. *Properties of Polymers*. Amsterdam: Elsevier. 875 pp.

Annual Review of Chemical and Biomolecular Engineering

Volume 2, 2011

Contents